

Angular Integration Autocorrelation Approach for Shear Wave Speed Estimation in the Framework of Reverberant Shear Wave Elastography

Hamidreza Asemani
Institute of Optics
University of Rochester
Rochester, USA

hasemani@ur.rochester.edu

Gilmer Flores Barrera
Department of Biomedical
Engineering
University of Rochester
Rochester, USA

gflor10@ur.rochester.edu

Jannick P. Rolland
Institute of Optics
University of Rochester
Rochester, USA

rolland@optics.rochester.edu

Kevin J. Parker
Department of Electrical and
Computer Engineering
University of Rochester
Rochester, USA

kevin.parker@rochester.edu

Abstract—Reverberant Shear Wave Elastography (RSWE) is a novel imaging modality with promising outcomes across various clinical applications. The current estimation approach assumes a significantly isotropic distribution of the shear waves within the medium, which may not be achieved in all cases. Therefore, this study proposes the Angular Integration Autocorrelation (AIA) approach that calculates the angular average value around the 2D autocorrelation, producing a robust single 1D function of radial lag for efficient estimation of local wavenumber and SWS. The effectiveness of the AIA estimator for SWS estimation is first validated using a k-Wave simulation of a stiff branching tube in a uniform background. To further evaluate the effectiveness of the AIA estimator, ultrasound elastography experiments are conducted across a range of different excitation frequencies on a breast phantom with a lesion. The results demonstrate that compared with simple autocorrelation approaches, the AIA estimator improves both the accuracy of the estimated SWS and the signal-to-noise ratio (SNR) in estimating SWS.

Keywords— shear wave elastography, reverberant shear wave, autocorrelation estimator, ultrasound elastography

I. INTRODUCTION

Reverberant Shear Wave Elastography (RSWE) represents a new approach to elastography that shows potential advantages across numerous clinical scenarios. It has demonstrated enhanced accuracy and resolution compared to earlier estimators in diverse tissues like the breast, liver, cornea, and brain using multiple external vibration sources [1-4]. The simplest estimation involves calculating the 2D autocorrelation of the particle velocity and fitting the axial and lateral profiles with their corresponding theoretical functions to obtain the average local wavenumber and subsequently, the shear wave speed (SWS) [5]. This estimation approach assumes a significantly isotropic distribution of the shear waves within the medium, which may not be achieved in all cases. Therefore, this study proposes the Angular Integration Autocorrelation (AIA) approach that calculates the angular average value around the 2D autocorrelation, producing a robust single 1D function of radial lag for efficient estimation of local wavenumber and SWS.

II. MATHEMATICAL PRINCIPLES

A fully reverberant shear wave field can be described as the superposition of multiple planar shear waves propagating in arbitrary orientations with the same wavenumber k and angular frequency ω_0 . The scalar component of particle velocity in the z -direction for a fully reverberant shear wave field in an isotropic medium is defined as follows [6]:

$$V_z(\boldsymbol{\varepsilon}, t) = \sum_{q,l} n_{qlz} v_{ql} e^{i(k\hat{\mathbf{n}}_q \cdot \boldsymbol{\varepsilon} - \omega_0 t)} \quad (1)$$

where $\boldsymbol{\varepsilon}$ is the position vector, t describes time, the indices q and l represent realizations of the random unit vectors $\hat{\mathbf{n}}_q$ and $\hat{\mathbf{n}}_{ql}$, respectively, and n_{qlz} signifies the scalar component of $\hat{\mathbf{n}}_{ql}$ in the z -direction. In order to estimate the shear wave speed, or extract the wavenumber from equation (1), the autocorrelation estimator is typically employed. By utilizing the spherical coordinate system as defined by Aleman-Castañeda *et al.* [7], we derive the following expression for the autocorrelation of the velocity field in both space and temporal domains:

$$B_{V_z V_z}(\Delta\boldsymbol{\varepsilon}, \Delta t) = 3\bar{V}_z^2 e^{i\omega_0 \Delta t} \left\{ \frac{\sin^2 \theta_s}{2} \left[j_0(k\Delta\varepsilon) - \frac{j_1(k\Delta\varepsilon)}{k\Delta\varepsilon} \right] + \cos^2 \theta_s \frac{j_1(k\Delta\varepsilon)}{k\Delta\varepsilon} \right\} \quad (2)$$

where $B_{V_z V_z}(\Delta\boldsymbol{\varepsilon}, \Delta t)$ denotes the autocorrelation function, \bar{V}_z^2 represents the ensemble average velocity squared, θ_s signifies the angle of $\Delta\boldsymbol{\varepsilon}$ with respect to the sensor axis (considered as the z -axis), j_0 is the first kind spherical Bessel function of zero order and j_1 is the first kind spherical Bessel function of first order. Integrating the autocorrelation function angularly across a two-dimensional plane spanning from 0 to 2π yields the subsequent expression:

$$B_{AIA_{zz}}(\Delta\rho, \Delta t) = \frac{3}{4} \bar{V}_z^2 e^{i\omega_0 \Delta t} \left[j_0(k\Delta\rho) + \frac{j_1(k\Delta\rho)}{k\Delta\rho} \right] \quad (3)$$

where $B_{AIA_{xz}}(\Delta\rho, \Delta t)$ represents the AIA function within the xz plane and $\Delta\rho$ denotes the one-dimensional shift (or lag) in the autocorrelation argument after integration around θ_s .

III. K-WAVE SIMULATION

The effectiveness of the AIA estimator for SWS estimation was initially validated using an elastography simulation. We conducted simulations involving the generation of a $120 \times 120 \times 120$ mm³ cube featuring an isotropic homogenous background with an isotropic y-shaped stiffer inclusion and random point sources vibrating at 200 Hz. The background exhibited a SWS of 1 m/s, while the inclusion boasted a higher SWS of 2 m/s. A fully reverberant shear wave field at a frequency of 200 Hz was generated in the medium by employing multiple excitation sources positioned randomly near the boundaries of the simulated medium. The particle velocity field along the z-axis is illustrated in Fig. 1(a). To enhance computational efficiency, we selectively trimmed the 3D Region of Interest (ROI).

Simple autocorrelation estimators in the x and z directions, as well as the AIA estimator in the xz plane, were applied to the shear wave field to estimate the SWS. Figs. 1(b) and 1(c) depict the SWS estimated using the simple baseline autocorrelation approaches in x -direction and z -direction, respectively. Fig. 1(d) showcases the estimated SWS using AIA in the xz plane. The mean SWS in the y-shaped tube using simple autocorrelation approaches in the x -direction and z -direction was estimated to be 2.08 m/s and 1.68 m/s (resulting in 4% and 16% estimation errors, respectively), while it was 1.98 m/s (with a 1% estimation error) using AIA. On the other hand, the signal-to-noise ratio (SNR) of the SWS in the background was estimated to be 9.62 dB for AIA, while it was 5.56 dB and 9.50 dB for simple autocorrelation approaches. These results clearly demonstrate that the AIA approach significantly enhances SWS estimation and effectively highlights the y-shaped tube against background.

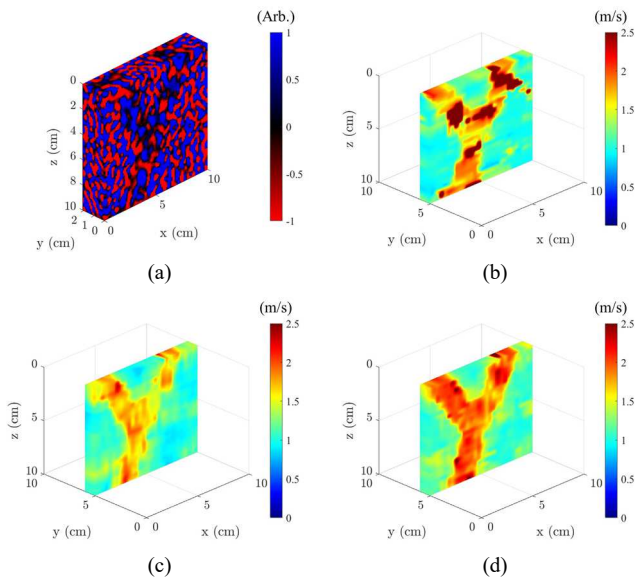


Fig. 1. k-Wave elastography simulation, (a) particle velocity field along the z-axis at the frequency of 200 Hz, (b) estimated SWS map using the simple autocorrelation approach in the x-direction, (c) estimated SWS map using the simple autocorrelation approach in the z-direction, (d) estimated SWS map using the AIA approach.

IV. ULTRASOUND ELASTOGRAPHY

In addition, practical experiments were conducted using a CIRS breast phantom (model 509, CIRS Inc., Norfolk, Virginia, USA) and a Verasonics scanner (V-1, Verasonics Inc., Kirkland, WA, USA) [3, 5]. The phantom model featured a 10 mm diameter lesion, and the acoustic field was generated by four vibration sources operating at 400, 600, and 900 Hz. The phase map of the shear wave field at the frequency of 900 Hz is presented in Fig. 2(a). Figs. 2(b), 2(c) and 2(d) illustrate the estimated SWS using simple autocorrelation approaches in x and z directions and the AIA approach, respectively. The mean SWS in the background, using simple autocorrelation approaches in the x -direction and z -direction, was estimated to be 2.49 m/s and 3.47 m/s, respectively, while it was determined to be 2.45 m/s using AIA. Considering the reported value of 2.27 m/s in [3] as the ground truth, the SWS estimation error at a frequency of 900 Hz for simple autocorrelation approaches and AIA are calculated to be 10%, 65%, and 8% respectively. On the other hand, the SNR of the SWS in the background was estimated to be 13.38 dB for AIA, while it was 11.73 dB and 5.36 dB for simple autocorrelation approaches, indicating a 14% and 150% improvement over simple autocorrelation estimations. Similar results were obtained at the excitation frequencies of 400 Hz and 600 Hz, as shown in TABLE 1.

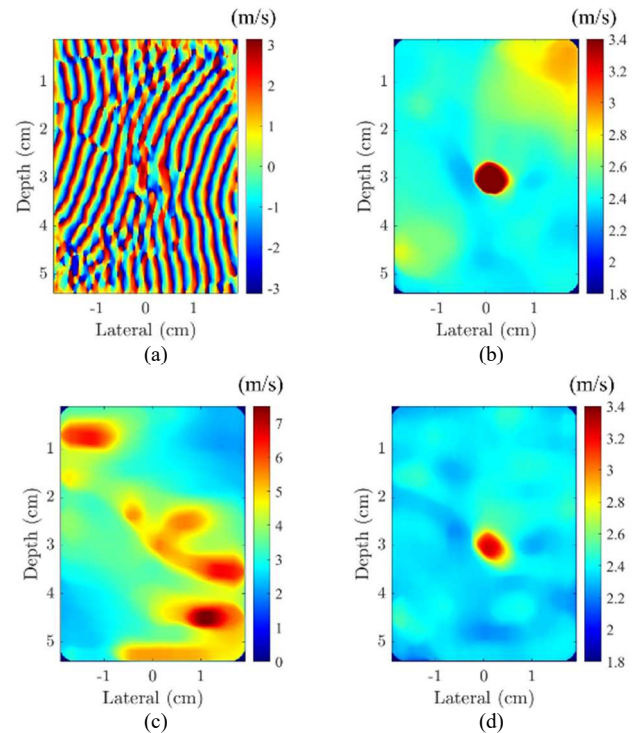


Fig. 2. Ultrasound elastography of breast phantom with a lesion, (a) phase map of the shear wave field at the frequency of 900 Hz, (b) estimated SWS map using the simple autocorrelation approach in the x-direction, (c) estimated SWS map using the simple autocorrelation approach in the z-direction, and (d) estimated SWS map using the AIA approach.

TABLE 1. SNR COMPARISON OF ESTIMATED SWS IN THE BACKGROUND FOR BREAST PHANTOM ULTRASOUND ELASTOGRAPHY: AIA APPROACH VS. SIMPLE AUTOCORRELATION APPROACHES AT VARIOUS EXCITATION FREQUENCIES.

Excitation frequency	SNR (dB) in background using simple autocorrelation (k_x)	SNR (dB) in background using simple autocorrelation (k_z)	SNR (dB) in background using AIA	AIA improvement over k_x	AIA improvement over k_z
900 Hz	11.73	5.36	13.38	14%	150%
600 Hz	12.49	5.66	13.01	4%	130%
400 Hz	12.35	6.43	12.44	1%	93%

V. CONCLUSION

In this study, we introduced the angular integral autocorrelation estimator for elastography measurements. The results of this study demonstrate the robustness of the proposed advanced autocorrelation estimator in differentiating between tissues with varying stiffness. Our contributions can be summarized as follows:

- Improved estimator through integration over all directions of 2D autocorrelation function.
- Major improvement over earlier approaches when estimating imperfect reverberant fields.
- Major improvement in SNR across a wide range of experiments, and shear wave frequencies.

ACKNOWLEDGMENT

We gratefully acknowledge the support provided by National Institutes of Health (Grant number: R21AG070331) and the University of Rochester Center of Excellence in Data Science for Empire State Development (Grant number: 2089A015).

REFERENCES

- [1] F. Zvietcovich, P. Pongchalee, P. Meemon, J. P. Rolland and K. J. Parker, "Reverberant 3d optical coherence elastography maps the elasticity of individual corneal layers," *Nat. Commun.* vol. 10, pp. 4895, 2019.
- [2] G. R. Ge, W. Song, M. Nedergaard, J. P. Rolland and K. J. Parker, "Theory of sleep/wake cycles affecting brain elastography," *Phys. Med. Biol.* vol. 67, pp. 225013, 2022.
- [3] J. Ormachea, and K. J. Parker, "Reverberant shear wave phase gradients for elastography," *Phys. Med. Biol.* vol. 66, pp. 175001, 2021.
- [4] I. E. Kabir, D. A. Caban-Rivera, J. Ormachea, K. J. Parker, C. L. Johnson and M. M. Doyley, "Reverberant magnetic resonance elastographic imaging using a single mechanical driver," *Phys. Med. Biol.* vol. 68, pp. 055015, 2023.
- [5] K. J. Parker, J. Ormachea, F. Zvietcovich and B. Castaneda, "Reverberant shear wave fields and estimation of tissue properties," *Phys. Med. Biol.* vol. 62, pp. 1046-61, 2017.
- [6] K. J. Parker and B. A. Maye, "Partially coherent radiation from reverberant chambers," *J. Acoust. Soc. Am.* vol. 76, pp. 309-13, 1984.
- [7] L. A. Aleman-Castañeda, F. Zvietcovich and K. J. Parker, "Reverberant elastography for the elastic characterization of anisotropic tissues," *IEEE J. Sel. Top. Quantum Electron.* vol. 27, pp. 7201312, 2021.